Solutions of Stars Based on C_{60}. Structural Behavior As Revealed by Small Angle Neutron Scattering

Claude Picot, Fabrice Audouin, and Claude Mathis*

Institut Charles Sadron (CNRS−ULP), 6, rue Boussingault, 67083 Strasbourg, France

Received March 13, 2006; Revised Manuscript Received December 21, 2006

ABSTRACT: The conformation in dilute solution and the structural behavior in semidilute solutions of polystyrene-substituted fullerene stars (StH) have been investigated using small-angle neutron scattering (SANS). Six-arm stars of low polydispersity and well-defined functionality ($f = 6$) have been synthesized by anionic polymerization with molecular weights covering nearly four decades ($7600 < M_{w,star} < 2040000$ g/mol). Stars with selectively H/D-labeled sequences linked to the fullerene core (StHD) have also been synthesized. SANS measurements have been performed in a wide range of scattering vectors ($0.002 < q$ (Å^{-1}) < 0.2). The single star scattering form factor $P(q)$ has been obtained from the scattering of highly dilute solutions by extrapolation at zero concentration. In the Guinier range of q, the measured molecular weight dependence of the radius of gyration R_g is found in close agreement with the results appearing in the literature on stars of different chemical structures and functionality. The form factor has been analyzed in the framework of scaling theories. Using the standard representation $P(q)$ as a function of qR_g, a good agreement has been observed in the Guinier and in the asymptotic ranges of q, but a significant discrepancy is noticed in the intermediate q range. The deviation is more and more pronounced as the arm length of the stars diminishes. That shows that, for stars with such a low functionality (six arms) the segment density profile suggested by the scaling theories is not really established. An identical behavior of the form factor is observed for selectively core-labeled stars in a solvent, matching the contrast of the outer sequences. Thus, it is shown that the variation of the arm length has no significant effect on the conformation of the arm segments attached to the core. A detailed analysis of the form factor of low molecular stars suggests that the scattering results from a shell of closely crowded extended chains. By matching the contrast of the outer arm sequences with the solvent, the structure factor $S_{int}(q)$ of selectively H/D-labeled stars has been studied in the case of volume fractions below and above the overlap concentration C^*. For stars with short arms, local ordering has been observed for low volume fractions (below C*), and the increase in concentration results in a more liquid-like inter-star spatial distribution. For stars with longer arms, a liquid-like spatial distribution is observed, whatever the concentration.

I. Introduction

Polymer-substituted fullerenes are attractive for the preparation of supramolecular assemblies of C_{60} and are well suited for the study of their physical properties. In fact, the main interest of polymer-substituted fullerenes is the improvement of their solubility and, therefore, their molecular dispersion in the bulk state. Among the different methods of grafting polymer on fullerene, the synthesis of stars by the addition of living anionic polymers on C_{60} is of special interest.[1−5] The addition mechanism of carbanions onto C_{60} is now well established[5,6] and offers a unique opportunity to control the molecular mass and polydispersity of the grafts, as well as the number of grafted chains. It has been shown that the delocalization of the carbanions introduced on the conjugated C_{60} molecule upon addition of "living" polymers, like polystyryl−Li, limits to a maximum of six the number of grafted chains.[5−7] This method provides an easy synthetic route toward well-defined model particles consisting of a hard spherical core (C_{60}) bearing six chains, whose degree of polymerization can be varied in a wide range. In the present study, a series of six-arm fullerene stars has been synthesized with the degree of polymerization of the arms covering more then 3 decades (12−3400). This offers a unique opportunity to, carefully and systematically, characterize the behavior of these well-defined branched objects as a function of their size. Small-angle neutron scattering (SANS) has been shown to be an appropriate technique for the characterization of star polymers. Most of the experiments reported in the literature have been carried out on stars of different chemical structure (PI, PB, PS) and functionality. The conformation in dilute solutions, as well as the structural behavior in semidilute solutions, has already been extensively investigated.[8−15] Nevertheless, the influence of the arm length of the stars has not been systematically studied and the range covered by the arm's molecular weights seldom exceeded one decade. More recently, SANS has been applied to study the structure of polymer-substituted fullerene.[16−21] However, in these experiments, the number of arms linked to the C_{60} or their length were not precisely defined. The work presented here has the advantage of focusing on a set of well-defined six-arm C_{60} stars, covering a very broad range of molecular weights ($1200 < M_{w,arm} < 340\,000$ g/mol), and characterized by SANS experiments carried out in a wide range of scattering vectors. The behavior of C_{60} polystyrene stars (StH) in dilute solutions of a good deuterated solvent (e.g., toluene-d_8) and within the zero concentration limit has been investigated. The variation of the static radius of gyration has been analyzed as well as the effect of excluded volume on the internal structure of the stars. The results have been compared to those reported in the literature. The scattering form factor has been discussed in the framework of existing theories, particularly the scaling approach.[22] In order to have a direct insight into the internal structure of a star in the vicinity of the fullerene core, SANS measurements have been performed on H/D labeled stars (StHD), in deuterated solvents matching the contrast of the terminal PSD sequence of the arms. Both good solvent and Θ conditions have been considered (e.g., dioxane-d_8 and cyclohexane-d_{12}). The structure factor of C_{60}

10.1021/ma060557k CCC: $37.00
Published on Web 02/10/2007

polystyrene stars in semidilute solutions in a good solvent (dioxane-d_8) has been analyzed by performing SANS measurements on core labeled stars (StHD). The influence of the arm length on the structural ordering has been evidenced by investigating concentrations close and far above the overlapping concentration of the StHD stars.

II. Experimental Section

1. Sample Preparation and Characterization. All polymers used in this work were prepared by anionic polymerization and the experiments were conducted in glass apparatus sealed under high vacuum, using the break-seal technique.[23]

Purification of Solvents, Monomers, C_{60}, and Initiator. Toluene free of protonic impurities was distilled through a vacuum line, directly into the apparatus, from a red solution of 3-methyl-1,1-diphenylpenthyllithium. Styrene and styrene-d_8 (Aldrich) were distilled twice over sodium wire, under controlled atmosphere, and then distilled under high vacuum from a solution of *n*-butyllithium (prepolymerization) directly in ampoules equipped with break-seals. C_{60} (>99% from SES Research) was stirred several hours in pure THF and recovered by centrifugation. This procedure was repeated until the THF remained colorless. The C_{60} was then dried under high vacuum ($<10^{-5}$ Torr) at about 150 °C, kept and handled under argon in a glove box. *sec*-Butyllithium (*sec*-BuLi) was prepared by reacting 2-chlorobutane with lithium metal in cyclohexane, and its concentration was determined by titration.

Synthesis of "Living" Polystyrenes and of Block Copolymers PS_D-*b*-PS_H, and Grafting onto C_{60}. "Living" polystyrenes (PS) were prepared by anionic polymerization in toluene, at room temperature, using *sec*-BuLi as initiator. The PS_D-*b*-PS_H block copolymers were obtained by adding styrene after complete polymerization of the deuterated styrene-d_8, and the ratio PS_H/PS_D adjusted by the respective amount of each monomer. The six-arm stars $(PS)_6C_{60}$ and $(PS_D$-*b*-$PS_H)_6C_{60}$ were prepared by reacting C_{60} with respectively PS−Li and PS_D-*b*-PS_H−Li in a 1:8 ratio according to the method described earlier.[5] In order to avoid any electron transfer from the terminal carbanion to the fullerene during this addition reaction it is necessary to prepare the "living" PS in a nonpolar solvent:[5] toluene was selected because of the relatively good solubility of C_{60} in this solvent.[24] The excess of ungrafted chains was removed from the hexa-adducts by classical polymer fractionation.

The molecular weights and the polydispersities of arms and stars were determined by using multiple detector size exclusion chromatography (SEC) and light scattering (LS). The SEC setup consisted of a Shimadzu LC10AD pump, an ERMA ERC3512 on-line degasser, a Waters automatic injector and five 300 × 7.5 mm PL Gel columns from Polymer Laboratories (4 × 10 μm Mixed-B and one 500 Å) connected in series. In addition to the refractive index (RI) detector (Shimadzu RID10A), a UV−vis detector (Shimadzu SPD10A) set at 320 nm was used to selectively detect the polymers including C_{60}. Indeed, at that wavelength, the PS is no longer detected, but the fullerene containing molecules absorb light. SEC is based on the variation of the hydrodynamic volume of the polymers with molecular weight, and needs calibration. It is well-known that the hydrodynamic volume of a star-shaped macromolecule is lower than that of the linear polymer of a same mass, and that the difference depends on the number of arms.[14] Due to the lack of appropriate standards for star polymers, calibration was done by using linear standards and, therefore, SEC was unable to provide the actual molecular weight of the star-shaped molecules. To determine the actual molecular weight of such branched macromolecules, an on-line light scattering detector (MALLS DAWN DSP from Wyatt Technology) was used. In addition, classical light scattering measurements were made using a FICA 50 apparatus. The light source was a 3 mW He−Ne laser (λ = 633 nm). The Zimm plot method was used to determine the weight-average molecular weight M_W and the radius of gyration R_G. For $(PS)_6C_{60}$ stars of a molecular weight above about 50000 g/mol, the contribution of the fullerene core becomes negligible, which is why the refractive index increment dn/dc of PS in THF solutions ($dn/dc = 0.186$ cm^3.g^{-1}) was used.[7] It should be noted that for the $(PS)_6C_{60}$ stars of very low molecular weights (samples StH1 and StH2 in Table 1), the absorption of the fullerene core at the wavelength of the light source (λ = 633 nm) cannot be neglected and, that therefore, the measured molecular weights for such samples are inaccurate.

Table 1. Size Exclusion Chromatography (SEC) and Light Scattering (LS) Characterization of the Six-Arm Stars and Their Arms, Where the Average Molecular Weights Are in g/mol and the Experimental Value for the Star Functionality Is $f = M_{wLS}$(star)/M_{wLS}(arm)

sample		SEC (RI detector)			LS	
		M_n	M_w	I	M_{wLS}	f
StH1	arm	1250	1350	1.08		
	star	7000	7600	1.09		
StH2	arm	3400	3500	1.03		
	star	17 600	18 900	1.07		
StH3	arm	8900	8500	1.05	9200	
	star	37 500	36 000	1.04	57 000	6.2
StH4	arm	17 600	18 300	1.04	17 800	
	star	78 000	85 000	1.09	105 000	5.9
StH5	arm	32 500	34 000	1.04	33 500	
	star	131 000	141 000	1.08	200 000	6.0
StH6	arm	86 000	90 000	1.05	88 000	
	star	362 000	396 000	1.09	536 000	6.1
StH7	arm	220 000	240 000	1.09	205 000	
	star	860 000	940 000	1.09	1200000	5.9
StH8	arm	310 000	360 000	1.16	347 000	
	star	1120000	1290000	1.15	2040000	5.9

Table 2. Size Exclusion Chromatography and Light Scattering Characterization of the Six-Arm $(PS_D$-*b*-$PS_H)_6C_{60}$ Stars and Their Block Copolymer PS_D-*b*-PS_H Arms

sample		SEC (RI detector)			LS			
		M_n	M_w	I	M_{wLS}	f	M_{wD}	M_{wH}
StHD1	arm	8400	7900	1.06	10 100		8200	1900
	star	35 000	38 000	1.09	64 000	6.3	49 000[a]	11 400[a]
StHD2	arm	18 000	19 200	1.07	22 000		18 500	3500
	star	83 000	79 000	1.05	127 000	5.8	111 000[a]	21 000[a]
StHD3	arm	46 000	43 000	1.07	44 000		41 000	3000
	star	227 000	214 000	1.06	260 000	5.9	246 000[a]	18 000[a]
StHD4	arm	40 000	42 000	1.05	46 000		39 000	7000
	star	171 000	161 000	1.06	270 000	5.9	234 000[a]	42 000[a]

[a] M_{wD} and M_{wH} for the six-arm stars were calculated from the D and H content in the arm.

The data are collected in Tables 1 and 2, along with the experimental star-functionality f ($f = M_{w,star}/M_{w,arm}$) for the stars with molecular weights high enough to be accurately measured by LS. For the sake of clarity, the samples $C_{60}(PS)_6$ and $(PS_D$-*b*-$PS_H)_6C_{60}$ have been respectively referenced in the tables as StH and StHD. In the discussion, the $(PS_D$-*b*-$PS_H)_6C_{60}$ samples will also be called "selectively labeled" or "core labeled" stars.

2. SANS Experiments. Neutron scattering experiments were conducted on the PACE spectrometer at Leon Brillouin Laboratory (LLB CEA Saclay, France), and on the D11 instrument at the Institute Laue Langevin (ILL Grenoble, France). Combinations of different neutrons wavelengths (λ = 5 and 7.6 Å) and sample−detector distances were used in order to cover a scattering vector (q) range from 0.002 to 0.2 Å^{-1}. The solutions were kept in quartz cells with a path length of 1 or 2 mm, depending on the transmission of the solution. According to standard procedure,[25] the scattering data were regrouped isotropicaly, and averaged at constant q values before normalization by the transmission and sample-thickness. Detector normalization was achieved with the flat incoherent scattering of water in identical experimental conditions. The incoherent contribution was subtracted by using a mixture of the solvent and a calculated amount of toluene corresponding to the incoherent contribution of the solute, so that each solution had its own appropriate background. Finally, absolute scattering cross sections were obtained by calibration with a water standard. As

Table 3. Scattering Length Densities ρ (10^{10} cm^{-2})[a]

	solute		
	styrene	styrene-d_8	C_{60}
	1.41	6.57	5.48
solvent	$\Delta\rho$	$\Delta\rho$	$\Delta\rho$
toluene-d_8 $\rho = 5.68$	−4.27	0.89	−0.2
dioxane-d_8 $\rho = 6.59$	−5.18	−0.02	−1.11
cyclohexane-d_{12} $\rho = 6.54$	−5.13	0.03	−1.06

[a] For C_{60}, ρ was calculated by assuming a radius of 5 Å and a density of 1.65 g cm^{-3}. These values come from experimental measurements.[17,44]

the aim of the scattering experiments was to cover a wide q range, the scattering measurements were carried out in different experimental configurations. In order to get the best junction between different configurations, the scattering has been recorded over a large overlapping range of q, both for the solutions and for the incoherent backgrounds.

Table 3 shows the scattering length densities of the species involved in the experiments as well as the contrast factor of the different systems of solute/solvent. The six-arm PSH stars were studied in toluene-d_8. In that case, the contrast factor of the C_{60} core appeared to be quite negligible compared to that of the styrene arms. Therefore, the contribution of the fullerene core should have no incidence on the scattering form factor of the star, as will be shown in the theoretical comments. Labeled stars $(PS_D\text{-}b\text{-}PS_H)_6C_{60}$ (samples StHD) were studied in dioxane-d_8, which perfectly matches the deuterated end-sequence of the arms. Some of these samples were studied in cyclohexane-d_{12} at 37 °C, corresponding to Θ conditions for the short Styrene H-sequences anchored on the fullerene core,[26] while matching, as for dioxane-d_8, the deuterated end-sequences of the arms. As for the solutions in toluene-d_8, the contribution of the C_{60} core can be considered negligible.

The dilute solutions have been investigated in a range of concentrations far below the overlapping concentration defined by $C^* = N/R_{g,star}{}^3 = 3/4\pi(M_w/N_A)R_{g,star}{}^{-3}$ (g mL^{-1}) so as to minimize the intermolecular contributions to the scattering. N_A is Avogadro's number, N the number concentration per unit volume, M_w the weight-average molecular weight, and $R_{g,star}$ the gyration radius of the star molecule. Obviously, the domain of concentrations strongly depends on the molecular weight of the stars, as shown in Table 4. The values of C^*, corresponding to "good solvent" (C^*_{GS}) and Θ (C^*_Θ) conditions, have also been listed in this table. In the case of good solvent, it is the relation proposed by Grest et al.[14] for the variation of $R_{g,star}$ with molecular weight $R_{g\ star}(GS) = 0.0756\ M_{star}{}^{0.6}$ which has been used. In Θ condition, the radius of gyration for a six-arm star is related to that of the arm by $R_{g,star}{}^2 = 8/3\ R_{g,arm}{}^2$. So, by taking the molecular weight variation of linear polystyrene $(R_g{}^2/M)^{0.5} = 2.75 \times 10^{-9}$ cm,[27] the variation becomes $R_{g,star\ six\ arms}$ (Å) $= 0.183\ M_{star}{}^{0.5}$.

III. Basic Scattering Relations

In order to discuss the results of the scattering experiments on the systems considered, some basic theoretical concepts and formulations should be recalled[25] in order to identify the parameters made accessible by the experiments, as well as the conditions of their validity.

For particles with a potential interaction of spherical symmetry, the scattering cross section per unit volume can be written as follows:

$$\Sigma(q) = \Delta\rho^2 \Phi V_p P(q) S_{int}(q) \qquad (1)$$

Here q is the scattering vector given by $4\pi\ \sin(\theta/2)/\lambda$, θ the scattering angle and λ the wavelength. Φ is the volume fraction of the particles of dry volume V_P and $\Delta\rho$ the excess of scattering-length density. $P(q)$ and $S_{int}(q)$ represent the form factor of the particle normalized to unity for $q = 0$, and the interparticle structure factor. The latter expression is valid, within a good approximation, for solutions of centrosymetrical particles, such as like colloids, or for branched polymers, such as stars with a functionality at least equal to 6. On the other hand, it no longer applies to linear polymer solutions.

By introducing more practical experimental parameters, such as the concentration in weight per volume $C_{w/v}$, the specific volume of the scattering species υ_{sp} and the weight-average molecular weight M_w, $\Sigma(q)$ can be written as

$$\Sigma(q) = \frac{\Delta\rho^2 \upsilon_{sp}{}^2}{N_A} C_{w/v} M_w P(q) S_{int}(q) = (K/m)^2 N_A C_{w/v} M_w P(q) S_{int}(q) \qquad (2)$$

with $K = m\upsilon_{sp}\Delta\rho/N_A$ and m the molecular weight per scattering unit.

Relation 2 is similar to the expression used in light scattering, where the contrast per unit mass (K/m) is equivalent to the refractive increment index.

The challenge is then to unambiguously characterize, by appropriate experiments, the form-factor $P(q)$ and the spatial correlation function $S_{int}(q)$ of the dispersed particles. The determination of $P(q)$ can be discussed for different levels of concentrations.

In the case of dilute solutions, and for weak particles interactions, $S_{int}(q)$ tends toward unity and $P(q)$ can be obtained by an extrapolation to zero concentration. For particles with short-range repulsive interactions in dilute solution, one introduces the second virial coefficient A_2 and the reverse of $\Sigma(q)$ is usually considered and is expressed by

$$\frac{\Delta\rho^2}{\Sigma(q)}\Phi = \frac{N_A}{V_w}\frac{1}{P(q)} + 2A_2\Phi \qquad (3)$$

where V_w is the weight-average molar volume of the particles.

In the small q range ($qR_g \ll 1$) the form-factor can always be written as $P(q) = (1 - q^2R_g{}^2/3)$ and the classical Zimm representation allows for the evaluation of the radius of gyration R_g and the second virial coefficient A_2.

At higher concentrations, the interparticle interactions cannot be taken into account only by the second virial coefficient A_2. Above the overlap concentration C^*, the polymers strongly interpenetrate each other so that the solution behaves like a sea of blobs. Measurement of the polymer form-factor can then be achieved by performing SANS experiments on solutions of mixtures of labeled and nonlabeled polymers, under zero average contrast conditions.[18] These experiments are very time-consuming and are generally performed for a precise determination of the variation of the polymer dimensions as a function of concentration. On the other hand, the determination of the structure factor $S_{int}(q)$ by a simple division of $\Sigma(q)$ by $P(q)$ in the zero concentration limit (see relation 2) is not justified because of the concentration dependence of the form factor.

1. Dilute Solutions: Form Factor of Star Polymers, Gaussian Statistics. Monocomponent Star Polymers. The form factor for monocomponent star polymer molecules composed of f arms has been calculated by Benoit[28] in the

Table 4. Experimental Parameters of StH and StHD Star Polymers (M_w Are Given in g/mol and R_g in Å), Where the Values of the Weight Average Molecular Weights Determined by Light Scattering Are within the Accuracy of This Technique

sample stars H/toluene-d_8	$M_{w,star}$ LS	$M_{w,star}$ SANS	C^*_Θ [b]	C^*_{GS} [b]	$R^{GS}_{g,star}$ LS [c]	$R^{GS}_{g,star}$ SANS	$R^\Theta_{g,star}$ SANS
StH 1	8100[a]	7700 ± 400	0.71	0.73		17	
StH 2	21 000[a]	20 500 ± 900	0.45	0.36		26	
StH 3	57 000	59 500 ± 3000	0.25	0.14		51	
StH 4	105 000	100 000 ± 5000	0.19	0.088		71	
StH 5	200 000	195 000 ± 9500	0.14	0.053		106	
StH 6	536 000	490 000 ± 24 000	0.084	0.024	197	192	
StH 7	1200000	1200000 ± 60 000	0.056	0.012	368	375	
StH 8	2040000		0.043	0.008	487	-	

sample stars HD/ dioxane-d_8	$M_{w,star}$ LS	$M_{w,star}$ SANS	C^*(HD)	C^*(H)	C^*(HD)	C^*(H)	SANS $R^{GS}_{g,star}$	SANS $R^\Theta_{g,star}$
StHD 1	(HD) 64 000		0.24		0.13			
	(H) 11 400	12 000 ± 600		0.55		0.48	23	
StHD 2	(HD) 127 000		0.17		0.072			
	(H) 21 000	22 000 ± 1200		0.43		0.32	30	29
StHD 3	(HD) 260 000		0.12		0.043			
	(H) 18 000	19 000 ± 950		0.46		0.36	28	
StHD 4	(HD) 270 000		0.12		0.041			
	(H) 42 000	40 000 ± 2000		0.30		0.18	50	41

[a] Due to the strong absorption of fullerene in the visible range of wavelength, the values reported here for small stars have been calculated on the basis of $M_{star} = 6M_{arm}$. [b] The calculation of the overlap concentrations is detailed in the text. [c] See ref 7.

framework of Gaussian statistics:

$$P^*(q) = \left[\upsilon - 1 + \exp(-\upsilon) + \frac{f-1}{2}[1 - \exp(-\upsilon)]^2\right] \quad (4)$$

where $\upsilon = q^2R_{g\ arm}{}^2 = q^2R_{g\ star}{}^2\ f/(3f-2)$, $R_{g\ arm}{}^2$ and $R_{g\ star}{}^2$ being respectively the mean square radii of gyration of the arms and the star. Therefore, $P(q)$ can be plotted, according to a standard representation, as a function of $qR_{g\ star}$ for stars with a identical number of arms. At high q values, $P(q)$ can be written as $P^*(q\rightarrow\infty) = 2/(f\upsilon) + (f-3)/(f\upsilon^2)$ indicating that the typical q^{-2} Gaussian behavior in the asymptotic range is observed. This behavior, representing the correlations at short distances, is generally characterized by the classical Kratky representation of $q^2g(q)$, where $g(q) = n\ P^*(q)$ is the correlation function, n and b^2 the number and the mean square length of the statistical units of the arm ($R_{g,arm}{}^2 = nb^2/6$). The first term of the asymptotic expansion leads to $q^2g(q\rightarrow\infty) = 12/fb^2$ showing that, for a given functionality f, the Kratky plot exhibits a plateau which is independent of the length of the arm. This latter representation indicates a maximum at $qR_{g,star} = 2.23$ enabling the determination of $R_{g,star}$ from the experimental curve and this value can be compared, within a good approximation, with the one obtained in the Guinier range from the classical Zimm representation.

Up to now, it has been assumed that the chains obey Gaussian statistics. For polymers in good solvent, the excluded volume (e.v.) effect modifies the mean square distance between two scattering elements that is now expressed by $r^2 = b^2z^{2\nu}$, where z is the number of statistical units and ν the Flory exponent 3/5. Benoit et al.[29] have shown that the asymptotic behavior of the structure factor can then be written in form similar to that for Gaussian chains, by replacing υ by υ^ϵ where $\epsilon = 1/2\nu$ and introducing new constants. Consequently, for star polymers in good solvents, $g(q)$ should exhibit a common $q^{-5/3}$ asymptotic decrease, independent of the molecular weight. The generalized Kratky representation $q^{-5/3}\ g(q)$ is then generally used for probing the local conformation of the attached chains.

Multicomponent Star Polymers. For bicomponent scattering particles made of species a and b of molecular weight M_a and M_b and a total molecular weight $M_w = M_a + M_b$, relation 2 can be generalized in the form[25]

$$\sum(q) = \bar{K}^2N_AC_{w/v}M_wP_{app}(q) \quad (5)$$

where $\bar{K}$ is an average contrast factor defined by

$$\bar{K} = \frac{K_aM_a + K_bM_b}{M_a + M_b} = xK_a + (1-x)K_b \quad (6)$$

K_a and K_b are the contrast factors of components a and b : $K_a = m_a\upsilon_a\Delta\rho_a$ and $K_b = m_b\upsilon_b\Delta\rho_b$. x and $(1-x)$ are the weight fraction of components a and b: $x = M_a/M_w$; $(1-x) = M_b/M_w$. By introducing the relative contrast factors y and $(1-y)$ of parts a and b, $y = xK_a/\bar{K}$ and $(1-y) = (1-x)K_b/\bar{K}$, the apparent form factor normalized to unit $P_{app}(q)$ is defined by

$$P_{app}(q) = \{y^2P_a(q) + (1-y)^2P_b(q) + 2y(1-y)P_{ab}(q)\} \quad (7)$$

$P_a(q)$, $P_b(q)$ are the form factors of components a and b. $P_{ab}(q)$ is a cross-correlation normalized term taking into account the correlation between scatterers of parts a and b.

This equation is equivalent to the expression of Ionescu et al.[30] In principle, by carrying out experiments with three different values of y, it is possible to determine separately the three functions $P_a(q)$, $P_b(q)$ and $P_{ab}(q)$.

In the particular case where one of the component is predominant (for instance a), one is often led to consider merely the contribution of this principal part. Under this condition, relation 5 is rewritten in the form

$$\sum(q) = K_a{}^2N_AC_{a,w/v}M_{app}P_{app}(q) \quad (8)$$

with

$$M_{app} = (\bar{K}/K_a)^2M_w \quad (9)$$

Let us now consider the experimental cases related to this work.

Selectively Labeled Stars. Selective labeling is currently achieved by deuteriation of determined sites or sequences of the stars. The SANS measurements reported in this paper have been carried out on solutions of stars with arms labeled by short

sequences (a) close to the core. By considering the simple case where the solvent matches the external part of the arms (b), the scattering will then result from the central polymer corona (a). In these conditions, the scattering cross-section reduces to $\Sigma(q) = (K_a/m_a)^2 N_A C_{a,w/v} M_{w,a} P_a(q)$. In dilute solution conditions, this type of experiment enables one to characterize the conformation of the inner part of the stars, which can then be compared with the conformation of a fully labeled star of equivalent arm length. As will be seen in the experimental section, the labeling of the central part of the stars is also of prime interest for the analysis of the structure factor in the semidilute regime.

Sphere Core Star Polymers. As C_{60} polymer stars are built on a quasi-spherical core, the well-defined geometry of the particle allows to precisely calculate its scattering form factor. The influence of the core has to be examined, especially in the case of short arms when their size becomes comparable to the radius R_S of the core.

The apparent scattering form factor of sphere core star polymers has been calculated by Kotaka[31] in order to interpret the light scattering by solutions of block copolymer micelles, and by Pedersen[32,33] for spheres with Gaussian chains attached. For *f*-arm stars the following expression is obtained:

$$P(q)_{SC\ star} = \frac{1}{(\Delta\rho_s + f\Delta\rho_a)^2}\{\Delta\rho_s{}^2 F_s{}^2(q) + \Delta\rho_a{}^2[fP_a(q) + f(f-1)P_{aa}(q)] + 2f\Delta\rho_s\Delta\rho_a P_{sa}(q)\} \quad (10)$$

where $\Delta\rho_s$ and $\Delta\rho_a$are the excess of scattering density of the sphere (s) and of the arm (a).

$F_S(q)$ is the classical scattering amplitude of the sphere $F_S(q) = (3[\sin(qR_s) - qR_s\sin(qR_s)])/(qR_s)^3$. $P_a(q)$ and $P_{aa}(q)$ are the normalized intra- and inter form factors of the arms $P_a(q) = 2/\upsilon^2[\upsilon - 1 + \exp(-\upsilon)]$ and $P_{aa}(q) = (\sin(qR_s)/qR_s)^2((1 - \exp(-\upsilon))/\upsilon)^2$, and $P_{sa}(q)$ is the form factor resulting from the cross-correlations between the sphere core and the arms $P_{sa}(q) = F_s(q)\,(1 - \exp(-\upsilon))/\upsilon)\,\sin(qR_s)/qR_s$. As for monocomponent stars, $\upsilon = q^2\,R_{g,arm}{}^2$. When the radius of the core R_S tends toward zero, $P(q)_{SC,stars}$ reduces to the $P^*(q)$ (eq 4) expression calculated by Benoit for simple star polymers.

In the small q range, by expanding $F_S{}^2(q)$, $P_a(q)$, $P_{aa}(q)$ and $P_{sa}(q)$ as a function of q^2 in eq 10 and assuming for $\Sigma(q)$ the Guinier expression $\Sigma(q) = \bar{K}^2 C_{w/v} N_A M_w\{1 - q^2\bar{R}_{ap}{}^2/3\}$, one defines the apparent mean square radius of gyration as

$$\bar{R}_{app}{}^2 = \frac{1}{(\Delta\rho_s + f\,\Delta\rho_a)^2}\left\{\Delta\rho_a{}^2\left[f\bar{R}_a{}^2 + 3f(f-1)\left(\bar{R}_a{}^2 + \frac{\bar{R}_s{}^2}{3}\right)\right] + \frac{3}{5}\Delta\rho_s{}^2\bar{R}_s{}^2 + 3f\Delta\rho_s\Delta\rho_a\left(\bar{R}_a{}^2 + \frac{8}{15}\bar{R}_s{}^2\right)\right\} \quad (11)$$

where $\bar{R}_s{}^2$ and $\bar{R}_a{}^2$ are respectively the mean square radii of gyration of the sphere core and the arms. For $\bar{R}_s{}^2 = 0$, this expression reduces to $\bar{R}_{g\ star}{}^2 = \bar{R}_b{}^2(3 - 2/f)$ which is similar to the expression given by Benoit[28] for simple stars.

2. Dilute Solutions: Form Factor of Stars with Excluded Volume Effect. The conformational properties of star polymers with excluded volume effect (i.e., in good solvents) is of considerable interest due to the important influence of the central part of the star where the density of the chain segments is very different from that of the outer part. Accordingly, a rigorous theoretical solution of this problem presents a high degree of complexity. Theoretical scaling approaches have been pioneered by Daoud and Cotton[22] and by Birshtein and Zhulina.[34,35] Renormalization group calculations[36] and numerical simulations[37−40] corroborate the Daoud−Cotton (D.C.) model at least in the dilute regime.

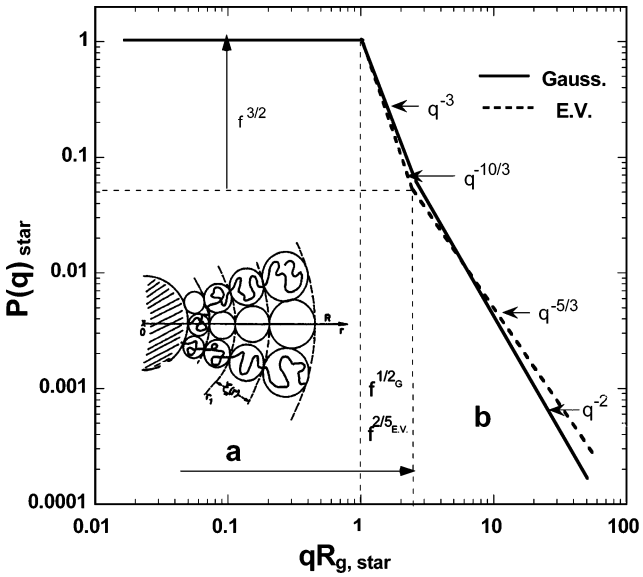

Figure 1. Form factor of star polymers in dilute solutions: (a) Daoud−Cotton model; (b) standard representation of the form factor.

In the D.C. model schematized in Figure 1a, the star consists of three regions. The central part is a melt like core where the tethered chains are highly close-packed and extended. The spatial extension of this region depends on the functionality *f* but is identical whatever the length of the arm. As the distance *r* from the center increases, the chain conformation is described first as a concentrated, then as a semidilute solution of blobs, characterized by an increasing screening length $\xi(r)$. The scaling regimes are defined by three characteristic lengths: the radius of the star R, the correlation length of the largest blob $\xi(R)$, and the monomer size σ. The blob size increases with the distance from the center as $\xi(r, f) \cong rf^{-1/2}$ and the polymer concentration is defined as $c(r) \cong f^{(1-\nu)/2} r^{(1-3\nu)/\nu}$ where ν is the excluded volume exponent ($^1/_2$ or $^3/_5$ for Θ and good solvent respectively). The D.C. model makes it then possible to predict the form factor $P(q)$ of the star with excluded volume effects. Following an approach proposed by Auvray and de Gennes[41,42] the form factor was calculated by Marques.[15] The characteristic lengths then define three ranges of scattering vector q. First, the Guinier range ($qR \ll 1$), where the form factor is defined by $P(q) \approx (1 - q^2R^2_{g,star}/3)$. Then, the intermediate range ($1 \ll qR \ll f^{2/5}$, $f^{1/2}$ for Gaussian statistics), where the form factor is the Fourier transform of the average concentration profile of the star. According to the model of Marques et al., the scattered intensity decreases, in this range, as $q^{-10/3}$ in the case of excluded volume, while it decreases as q^{-3} in the case of Gaussian statistics. Finely, the asymptotic range ($qR \gg f^{2/5}$) corresponding to the scattering of uncorrelated blobs, measures the intrachain correlation. It corresponds to the classical excluded volume behavior of an isolated chain, i.e., $q^{-5/3}$ or q^{-2} for Gaussian statistics.

These characteristic power law behaviors are depicted in Figure 1b, which also shows the position of the crossovers related to the star's functionality *f*, thus offering a check of the self-consistency of the experimental results. Finally, it must be underlined that the center-end distance of the star R is related to R_g measured in the Guinier range. The relation between these two parameters can be easily established in the framework of the D.C. model that leads to $\overline{R_g{}^2}/\overline{R^2} = {}^5/_{11}$ in the case of long arm chains in the swollen regime. This last value is comparable

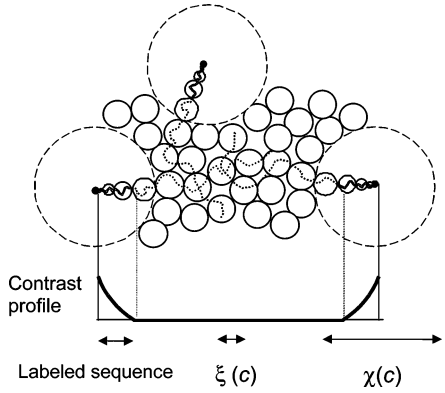

Figure 2. Schematic representation of a semidilute solution of star-shaped polymers (Daoud−Cotton model): (—) labeled chain sequences; (···) contrast matched chain sequences. The contrast profile *K* between two neighboring labeled stars is also represented.

to the results of Grest,[37] obtained by molecular dynamic simulation for stars of low functionality. By way of comparison, $\overline{R_g^2}/\overline{R^2} = {}^3/_5$ for a homogeneous dense sphere.

On the other hand, an approximate expression of the form factor, which describes reasonably well the results of the experiments, has been proposed by Dozier.[10] The correct behavior in the Guinier regime is described by Gaussian long-range correlations corresponding to the proper radius of gyration. The short-range correlations between monomer units are described by the classical correlation function of a single swollen chain with a cutoff function $\exp(-r/\xi)$ where ξ is the average blob size. It should be noted that this semiempirical approach does not take into account any increase in the blob size with its distance from the star center, therefore requiring an adjustment of fitting parameters.

3. Scattering by Semidilute Solutions of Star Polymers. According to the Daoud−Cotton model,[22] for concentrations above the overlapping concentration, the outer arms of the stars are interpenetrated and the solution is divided in two spaces of different structure as shown in Figure 2. In the region where the arms are interpenetrated, the star structure is no longer distinguishable, and the chain space distribution is comparable to a semidilute solution of linear chains with a blob size $\xi(c)$. Around the center of the star, there is a space of size χ where the star has a single star behavior. The structure of a semidilute solution of star polymers can then be described as a mixed structure of a dilute solution of stars of effective radius $\chi(c)$, imbedded in a matrix formed by the overlapping outer parts of the chains. As the concentration increases, $\chi(c)$ diminishes, while the space occupied by the sea of blobs increases. For much higher concentrations, the solution will be comparable to a concentrated solution of linear polymer chains. As for the form factor, since $\chi(c)$ decreases faster than $\xi(c)$ with the increase in concentration, the range of q^{-3} (or $q^{-10/3}$) power law behavior will shift to higher q values. Therefore, the q^{-2} (or $q^{-5/3}$) asymptotic decrease will move toward higher scattering vector values. These predictions are in agreement with available experimental data.[15] For sufficiently large values of the functionality, it as been shown by Witten[43] that for a semidilute star polymer solution, the osmotic pressure Π increases rapidly in the vicinity of C^*. This crossover in the concentration dependence of Π reveals strong interactions between neighboring stars. As a result, the scattered intensity will present a liquid peak corresponding to the star−star correlation $S_{int}(q)$. As mentioned earlier, this additional contribution to the scattering cross-section can be written as $\Sigma(q) \cong P(q)S_{int}(q)$, and it has been pointed out that the determination of $S_{int}(q)$ by a simple division of $\Sigma(q)$ by $P(q)$ is questionable. The characterization of $S_{int}(q)$ above C^* can be achieved more precisely by a (as punctual as possible) selective partial labeling of the central part of the star polymer (see Figure 2). Indeed, in the range of small scattering vectors, where $S_{int}(q)$ is strongly dependent on the overall polymer molecule interactions (long distances interactions), the form factor $P_{CL}(q)$ of core labeled stars will exhibit a negligible variation, compared to the total scattering form factor $P_T(q)$ of a fully labeled star. Therefore, the normalization of $\Sigma(q)$ by $P_{CL}(q)$ is justified. Another important point is that the overlapping concentration of the labeled part of the stars will be reached much later than that of the unlabeled species (in the experimental case presented here, the ratio is about 5 in the case of Gaussian statistics, but will evidently be much higher for stars with excluded volume) and so, the concentration effect on $P_{CL}(q)$ will be minimized. Furthermore, the scattering will not be affected by the sea of blobs of the overlapping chains. This labeling approach will be applied in the Experimental Section.

IV. Results and Discussion

1. $C_{60}(PS)_6$ Stars in Toluene-d_8 Dilute Solutions. The scattering behavior of a series of unlabeled six-arm PS stars (StH) with a C_{60} core and molecular weights covering three decades ($7300 < M_w < 1206000$ g/mol) has been investigated in toluene-d_8.

Figure 3 displays the variation of the scattering intensity at different concentrations for the lowest, intermediate and highest molecular weight investigated (StH1, StH4, StH7). The interparticle spatial distribution depends on the volume fraction of star polymers in the solution. Therefore, the concentration reference chosen here is the overlapping concentration C^*_{GS}. The values of C^*_{GS} listed in Table 4 have been calculated using the empiric law of molecular weight dependence of the radii of gyration of stars in good solvents proposed by Grest et al.[14] At low q, the graphs of Figure 3 show the strong contribution of the intermolecular correlation far below the overlapping concentration C^*_{GS}. As mentioned earlier, the analysis of the scattering cross section at a finite volume fraction is not obvious due to several contributions to the scattering. A precise determination of the structure factor would require SANS experiments under zero contrast conditions on solutions of mixtures of labeled and nonlabeled stars. As will be seen in a subsequent section, the case of semidilute solutions can be approached more directly, using core labeled stars. Consequently, this section will be mainly devoted to the study of dilute solutions. From the scattering intensities at different fixed low concentrations, the star form factor has been extrapolated to infinite dilution using a concentration dependent Zimm plot. This procedure was used in the Guinier regime and in the intermediate range of q. In the high q range, as was expected, the scattered intensities normalized by the concentration are superposed, supporting the consistency of the experimental measurements at different concentrations.

In the limit of $C_{w/v} \rightarrow 0$, relation 2 reduces to $\Sigma(q) = (K/m)^2 N_A C_{w/v} M_w P(q)$. As mentioned in the theoretical section, the scattering measurements on solutions of multicomponent particles lead to an apparent form factor, which depends on the relative contrast between the solute and the solvent (see relation 7). It then becomes important to compare the form factor of a simple star and that of a sphere core star under the experimental contrast conditions. In the case of Gaussian statistics, the structure factor of the smallest star ($M_{w,star} = 7300$, $f = 6$) has

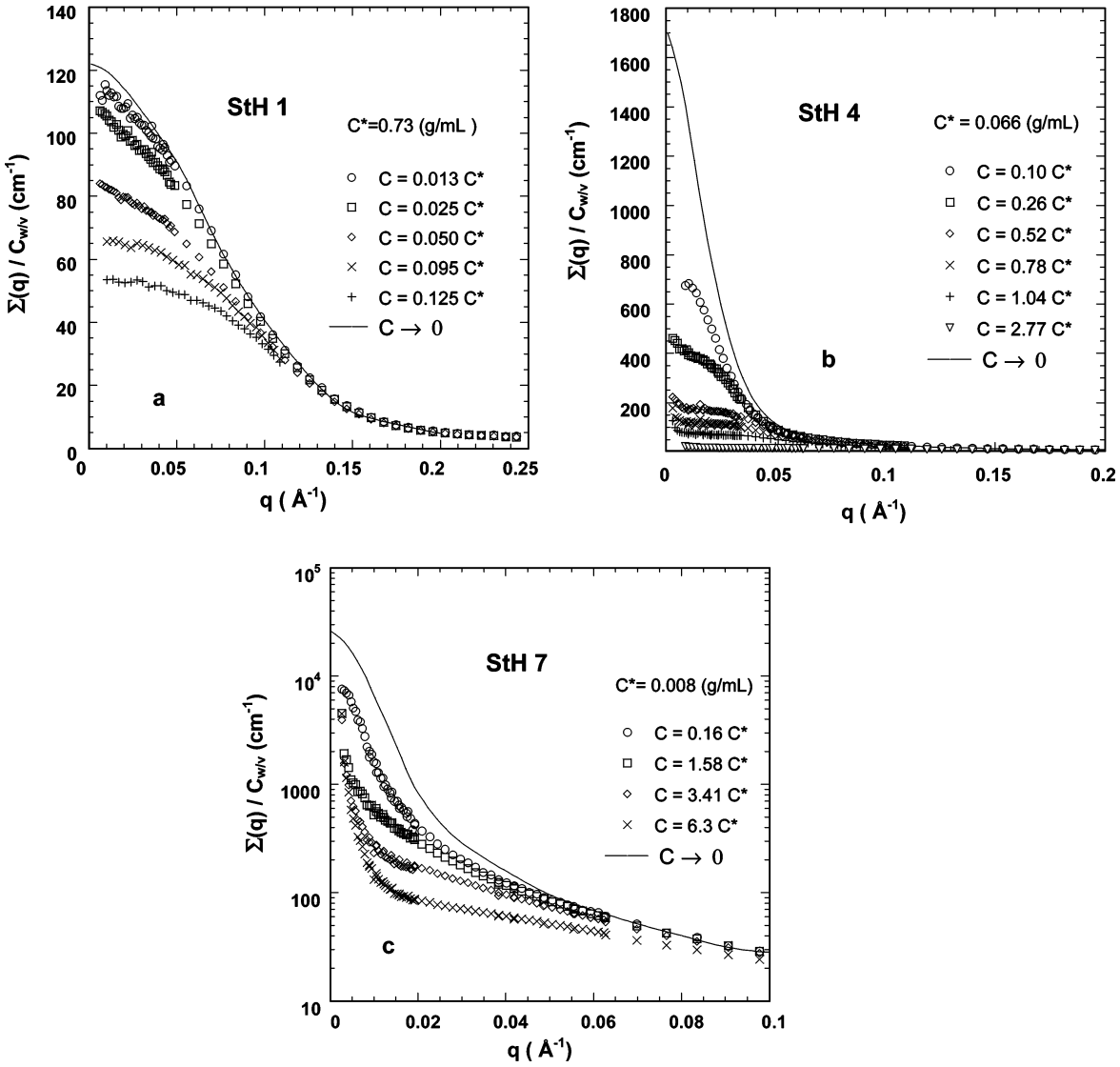

Figure 3. Solutions of StH stars in toluene-d_8: (a) StH1, M_w = 7600 g/mol; (b) StH4, M_w = 105000 g/mol; (c) StH7, M_w = 1200000 g/mol. Variation of the scattering intensity as a function of concentration.

been calculated using relations 4 and 10 and taking a radius of 5 Å for the fullerene core.[17,44] These calculations show that the contribution of the sphere C_{60} core does not contribute significantly to the star form factor.

Guinier Range of Scattering Vectors. In the Guinier range of scattering vectors ($q\,R_{g,star} < 1$) and in the limit of $C_{w/v} \rightarrow 0$ eq 3 can be written as

$$\frac{C_{w/v}K_{arm}{}^2}{\sum(q,C_{w/v}\rightarrow 0)} = \left(\frac{m^2}{N_A}\right)\frac{1}{M_w}\left(1 - \frac{q^2 R_{g\,star}{}^2}{3}\right) \qquad (12)$$

where m is the mass of the monomer unit.

Thus, by knowing the excess of scattering length density, a classical Zimm plot representation of the absolute scattering measurements allows the determination of the weight-average molecular weight M_w and of the radius of gyration for the different polymer stars. As an example, Figure 4 shows a concentration dependent Zimm plot for StH3.

In order to estimate more precisely the influence of the sphere core on the determination of the mean square dimensions of the stars, the ratio $(\bar{R}_{app}{}^2/\bar{R}_{g\,star}{}^2)^{1/2}$ was calculated using $\bar{R}_{g\,star}{}^2 = \bar{R}_{g\,arm}{}^2(3 - 2/f)$ and relation 11. It comes out clearly that the presence of the fullerene core does not affect significantly the determination of the mean dimensions in the range of molecular weights investigated. Only a slight difference (lower than 4%)

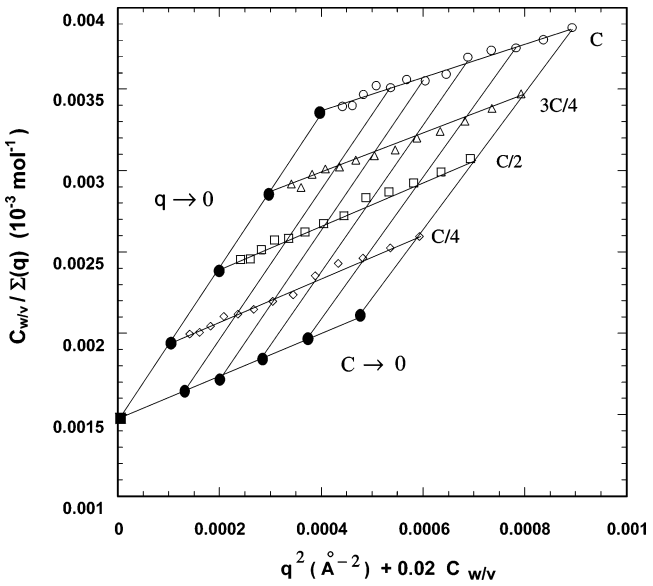

Figure 4. Concentration dependent Zimm plot of sample StH3 in toluene-d_8, C (w/v) = 1.94×10^{-2} gmL^{-1}.

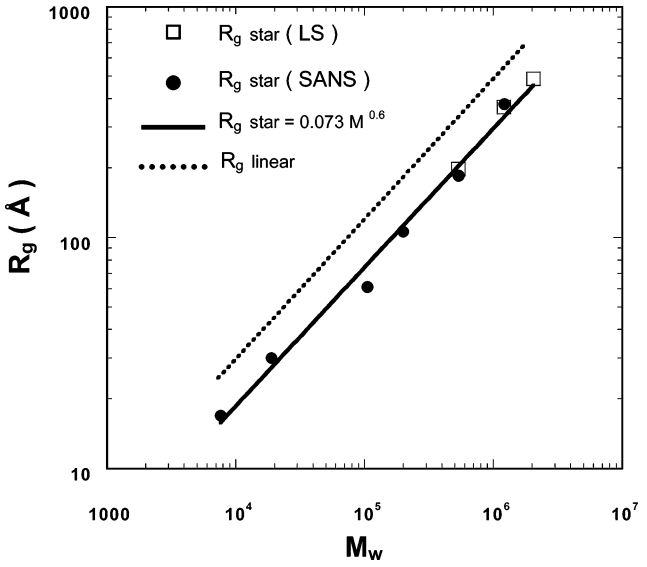

Figure 5. Variation of the radius of gyration as a function of the molecular weight: (●) SANS measurements; (□) light scattering measurements. Linear fit: (—) StH stars $(\overline{R_g^2})^{1/2} = 0.073M^{0.6}$; (---) linear polystyrene/toluene-d_8.

is revealed for the smallest star polymers, and that lies within the limits of experimental accuracy.

The same applies to the molecular weight determination. Relations 5 and 8 show that, by using either the average contrast factor $\bar{K}$ or that of the arms, the scattering cross section will be proportional to the total molecular weight of the multicomponent particle M_w or to the apparent molecular weight M_{app}. Relation 9 shows that $M_{app} = (K/K_{arm})^2 M_w$. It again comes out of the calculations that, for the set of stars investigated, the determination of the molecular weight is not noticeably affected, whether it is the average contrast factor or the contrast factor of the arms that is taken into consideration.

Although these evaluations have been discussed using the approximation of Gaussian statistics, they show that the polystyrene stars based on C_{60} can be considered as model stars with a punctual core in the scattering experiments described below. Accordingly, the molecular parameters, the molecular weight and the radii of gyration will be determined on the basis of mono-component polystyrene stars particles. However for stars with very short arms for which the dimension of the core becomes comparable to those of the anchored chains, the structure factor will be further discussed, taking into account the conformation of the chains close to the fullerene core.

The measured values of M_w are listed in Table 4 and compared to those obtained by light scattering.[7] Within an experimental precision of 5%, the agreement is quite satisfactory and confirms the reliability of the absolute neutron scattering measurements.

Beside the evaluation of the radii of gyration by SANS, R_g have been measured by light scattering for two samples (StH6 and StH7) of high molecular weight. The results included in Table 4 and in Figure 5 show an excellent agreement between the values obtained with these two different scattering techniques.

According to the scaling laws given by Daoud and Cotton in the dilute regime and for long arms stars, the dependence of $(R_g^2)^{1/2}$ on functionality f and on the number of statistical units per arm N_b is given by $(R_g^2)^{1/2} \sim N_b^{\nu} f^{(1-\nu)/2}$, where $\nu = {}^3/_5$ is the Flory exponent. By introducing the weight-average molecular weight of the star, one obtains for six-arm stars: $(R_g^2)^{1/2} = K(0.488)M_{w\,star}^{3/5}$. From a compilation of different experimental results, Grest et al.[14] have proposed master equations for the variation of the geometrical dimensions of several star polymers in solution as a function of their molecular mass. In the case of polystyrene star solutions in the good solvent limit, the prefactor K is given as 0.16, which leads for 6-arm stars to $(R_g^2)^{1/2} = 0.073M_{w\,star}^{0.6}$ in close accordance with our experimental results represented in Figure 5. It should be underlined that the experimental results reported here cover 3 decades of molecular mass.

Another interesting test for the consistency of the experimental results is a comparison of the size ratios for linear and star polymers. In a revue, Grest et al.[14] give a compilation of numerous experimental data for star polymers of functionality f ranging from 2 to 270. For six-arm stars these authors have reported a static ratio $(R_{g,\,star}^2/R_{g,\,arm}^2)^{1/2} = 1.9$ and 1.7, respectively for good solvent and Θ conditions. In Figure 5, the molecular weight dependence for the static dimensions of linear polystyrene in toluene $(R_{g,\,linear}^2)^{1/2} = 0.130M_w^{0.59}$, coming out from the experimental results of Rahlwes and Kirste,[45] is also plotted. The combination of this power law with our results leads to a static dimension ratio between stars and arms of 1.8 that matches, within the experimental precision, the outcome of the compilation by Grest et al.[14]

Regarding the molecular weight dependence of their overall dimensions, the polystyrene stars based on C_{60} exhibit a behavior quite comparable to that of polymer stars with different chemical structures. As a final remark, it should be noticed that, in spite of the weak coverage of the fullerene core by very short polystyrene arms, the consistency of the results of M_w and R_g confirms the conclusion that the dispersion of these PS stars with a C_{60} core remains monomolecular in dilute solution of toluene-d_8.

Analysis of the Form Factor. The variation of the mean square dimensions of polymer stars as a function of their arm length gives information about their overall geometric size dimensions. On the other hand, the analysis of the scattering form factor $P(q)$ enables a more detailed insight into the internal structure of the star polymers. From scattering measurements covering a wide q range, the form factor of the series of StH stars has been obtained by direct normalization of the scattering cross section $\Sigma(q)$ by $\Sigma(q=0)$; this last value was obtained from the Zimm plot extrapolation. This procedure permits a direct and consistent evaluation of $P(q)$ without the need to introduce external parameters like the contrast factor, the specific volumes, etc.

Figure 6a shows the molecular weight dependence of $P(q)$. The reliability of the normalization is justified by the convergence of $P(q)$ to unity at small q values, but also by the expected e.v. behavior $P(q) \sim q^{-5/3}$ in the asymptotic range of scattering vectors. Furthermore, using the M_w values evaluated in the small q range, the correlation functions $g(q) \sim M_w P(q)$ have been represented in Figure 6b. As expected in the asymptotic range, $g(q)$ exhibits the typical $q^{-5/3}$ decrease, independent of M_w. This last result again confirms the consistency between the results obtained in the small and in the high q range of scattering vectors, and supports the conclusion that the scattering indeed results from monomolecular dispersions of $C_{60}(PS)_6$ stars.

It has been outlined in the theoretical section that scaling the representation of $P(q)$ with R_g leads to a master curve for Gaussian stars of fixed functionality. Figure 7 displays the experimental results obtained for such a standard representation. The overlapping of the form factor is well observed in the Guinier range and in the asymptotic domain characterized by a

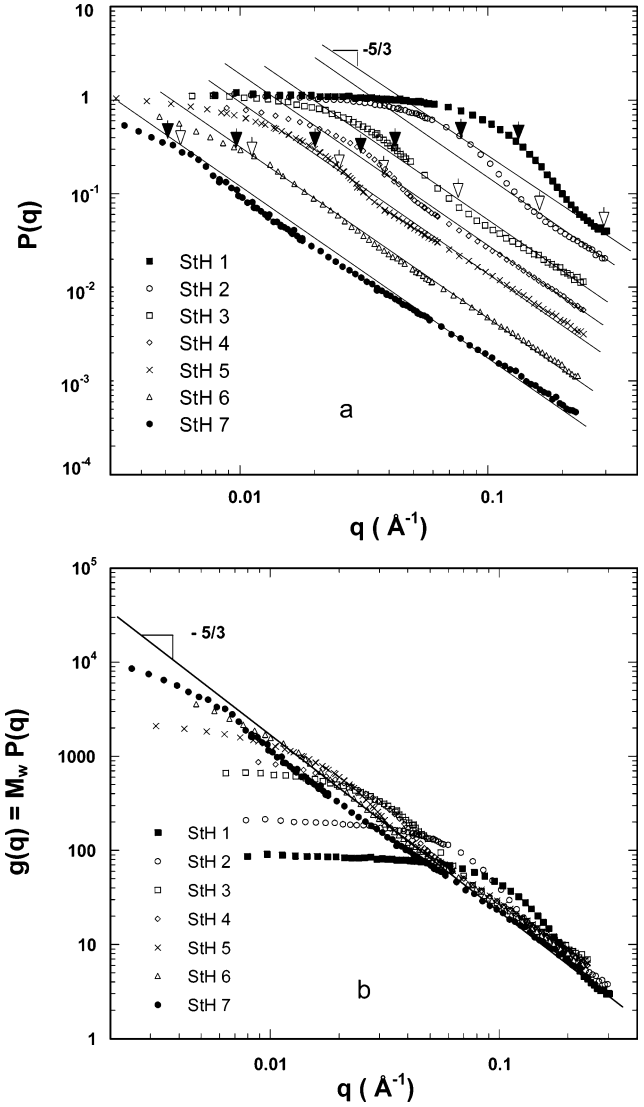

Figure 6. (a) Form factor $P(q)$ of six-arm fullerene stars. The arrows indicate the onset of the asymptotic regime. Filled symbols: calculated according to $qR_g \sim f^{1/2}$. Open symbols: experimental crossover. (b) Correlation function of six-arm stars $g(q) = M_wP(q)$.

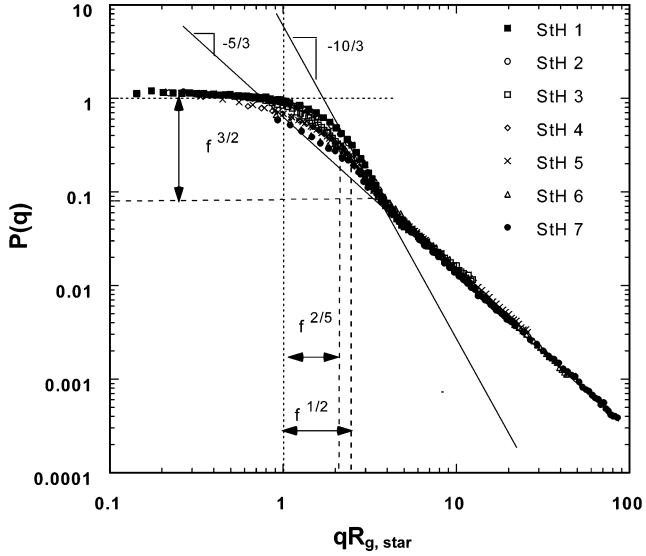

Figure 7. Standard representation of the form factor for six-arm C_{60}-polystyrene stars in dilute toluene-d_8 solution. The characteristic regimes predicted by the scaling theory are represented by there power law behavior in the corresponding domain of scattering vectors.

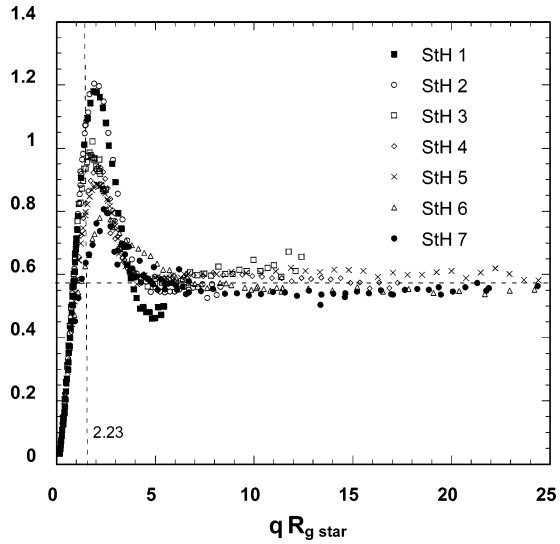

Figure 8. Generalized Kratky plot of StH stars in toluene-d_8 solution ($C \rightarrow 0$).

$q^{-5/3}$ decrease. But, in the intermediate range, $P(q)$ exhibits a hump all the more pronounced as the arm length decreases. As a reference, the $q^{-10/3}$ behavior predicted by the scaling theory has also been represented in this standard log−log representation. This observation indicates that, contrary to linear polymer chains, the six-arm stars diluted in good solvents cannot be regarded as self-similar objects.

The scaling analysis foresees that the fall of $P(q)$ from the Guinier range to the onset of the asymptotic behavior should be proportional to $f^{3/2}$. As can be seen in Figure 7, the experimental results exhibit the expected drop of intensity by a factor $f^{3/2} \cong 14.7$, within the precision of the determination of the onset of the asymptotic regime. This last regime is supposed to take place for qR_g values close to $f^{1/2}$ (Gaussian) or $f^{2/5}$ (e.v.). The standard representation shows that the observed onset of the asymptotic regime develops at higher values of qR_g, regardless of the star molecular weight. This discrepancy is better evidenced in Figure 6a, where the form factors of the stars with different molecular weights are represented together with the experimental and theoretical onsets of the asymptotic regime. The theoretical onset value has been calculated on the assumption that the break should occur at $q = f^{1/2}/R_g$. Moreover, it can be then pointed out that the discrepancy observed is even more pronounced as the length of the star arms decreases. These observations raise the question of the applicability of the scaling approach for six-arm stars and especially for short arm lengths. The observation that the intermediate regime extends to higher q values for short arm lengths suggest that, for these low functionality stars, the region surrounding the fullerene core extends on a spatial distance lower than that predicted by scaling approaches.

In Figure 8, the generalized Kratky representation shows more explicitly the evolution of the form factor as a function of the arm length. The maximum observed in the intermediate q range is positioned within the experimental accuracy at $qR_g = 2.23$ as expected for six-arm stars, but its amplitude increases as the arm length decreases. As mentioned in the theoretical part, the influence of the sphere core cannot be invoked to justify this evolution of the form factor, at least in the case of a Gaussian statistics. This argument is certainly justified in the case of stars with excluded volume effect. Therefore, the first interpretation that comes out of the experimental observations is that for stars with small molecular weight, the scattering results predominantly

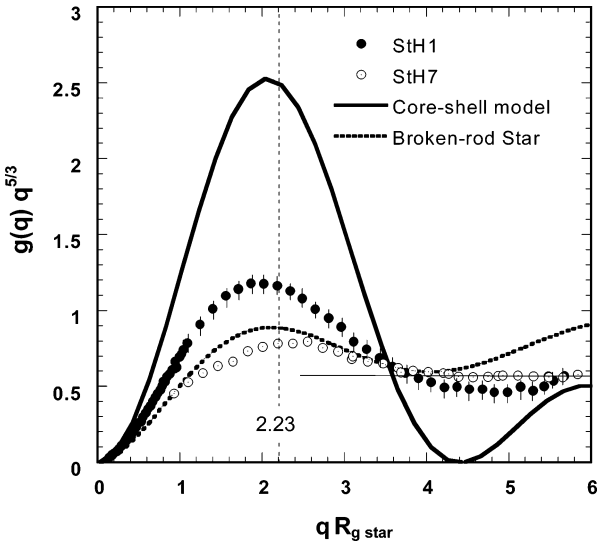

Figure 9. Comparison of the generalized Kratky plots of StH1 (○) and StH7 (●) in solution in toluene-d_8. The continuous and the dotted lines represent respectively the scattering behavior of a core shell particle and a broken-rod star with a radius of gyration equivalent to the one of StH1.

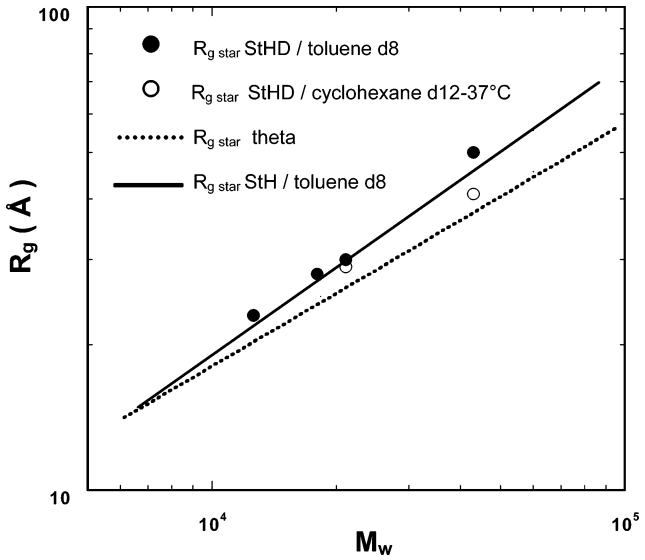

Figure 10. Variation of the radius of gyration of the central core of StHD labeled stars in dioxane-d_8 (●) and cyclohexane-d_{12} (○) solutions. For comparison the variation of R_g for StH stars in toluene-d_8 and the behavior in a Θ solvent have been also reported.

from a densification of the crowded short chains linked to the fullerene surface. At the opposite, for stars with long arms, the contribution to the scattering from the uncorrelated parts of the arms away from the core, dampens the scattering effect of the densification around the core of the star.

In order to get a better insight into the chain conformation at the vicinity of the core surface, the Kratky representations of the lowest and highest molecular weight stars (StH1 and StH7) have been represented in Figure 9, together with the scattering behavior calculated by using two extreme models for the short-arm star. The first one, where the C_{60} core is considered to be surrounded by a homogeneous shell of slightly swollen PS shell (core−shell model, C.S.),[25] is often used for the interpretation of the scattering by colloid suspensions. The corresponding scattering function, displayed in Figure 9, has been calculated using the experimental apparent radius of gyration of StH1 and the relevant scattering length densities of the inner and outer parts. The second model supposes a strong stretching effect of the grafted chains close to the star core. That arises from the fact that the chains are closely linked to a rather well-defined sharp boundary. This effect has already been revealed by the SANS experiments of Richter et al.[9] on 12-arm Polyisoprene stars. The broken-rod star model (B.R.) developed by Burchard et al.[46] has been used to account for this stretching effect. This model assumes that the arms are rods freely jointed to the star center. The corresponding generalized Kratky plot, represented in Figure 9, has been drown up by adjusting the rod length L of the arm ($L = 20$ Å) to respect the experimental value of the radius of gyration.

Several comments can be raised about these different representations. The generalized Kratky plot of StH7 ($M_w = 1200000$) does not show any peculiar behavior compared to that of stars with long arms in the good solvent situation. The asymptotic characteristic plateau is clearly reached and the position of the maximum of week amplitude is observed within a good approximation near $qR_g = 2.23$. Regarding the scattering behavior of StH1 ($M_w = 7600$), the amplitude of the characteristic maximum is more accentuated. A shallow minimum, followed by the beginning of a maximum, appear at higher qR_g values. Referring to the C.S. and B.R. models, it should be pointed out that the amplitude of the experimental maximum of StH1 lies between those of the two models, but closer to that of the B.R. model. Obviously, the core−shell model represents the extreme situation of a homogeneous compact shell that is somewhat unrealistic. Looking at the asymptotic behavior, it appears that the experimental position of the week minimum of sample StH1 lies closer to that of the C.S. model, which is an indication of the compactness of the arms in the vicinity of the core. Together these observations suggest that the very sharp boundary of the C_{60} core results in a close packing of stretched arms close to the core of these model stars.

Although based on qualitative arguments, this discussion brings out the basic differences between the chain conformation of stars with short and long arms. Undoubtedly, more careful scattering measurements in the high q range are needed in order to have a more precise insight into the conformation of isolated labeled chains linked to the core surface.

2. Selectively Labeled Stars (StHD) in Dioxane-d_8 and Cyclohexane-d_{12}. For these selectively labeled stars, the outer deuterated sequences of the arms is contrast matched by the solvent, and the aim of these experiments was 2-fold:

(i) First was to analyze the conformation of the central labeled part of the stars as a function of its size and of the length of the attached matched chains; these experiments are relevant to the dilute regime.

(ii) Second was to characterize the spatial distribution of the core labeled stars working at higher volume fraction of stars.

2.1. Dilute Solutions. Considering the strong spatial interaction between the contrast matched end sequences, it is important to underline that, for experiments in the dilute regime, it is the overlapping concentration C^*_{StHD} of the entire star that has to be taken into account as the reference. In Table 4, the different labeled stars investigated are listed, and the important difference between the overlapping concentration of the entire star and its labeled part is pointed out. Accordingly, as for StH stars, the scattering form factor of the central labeled core has been obtained, by extrapolation at zero concentration, from scattering intensities recorded far below C^*_{StHD}. In dilute solution, $\chi(c)$ is much larger than the radius of the central labeled part of the star (see Figure 2).

Guinier Range of Scattering Vectors. The weight-average molecular weight of the H labeled core has been estimated from

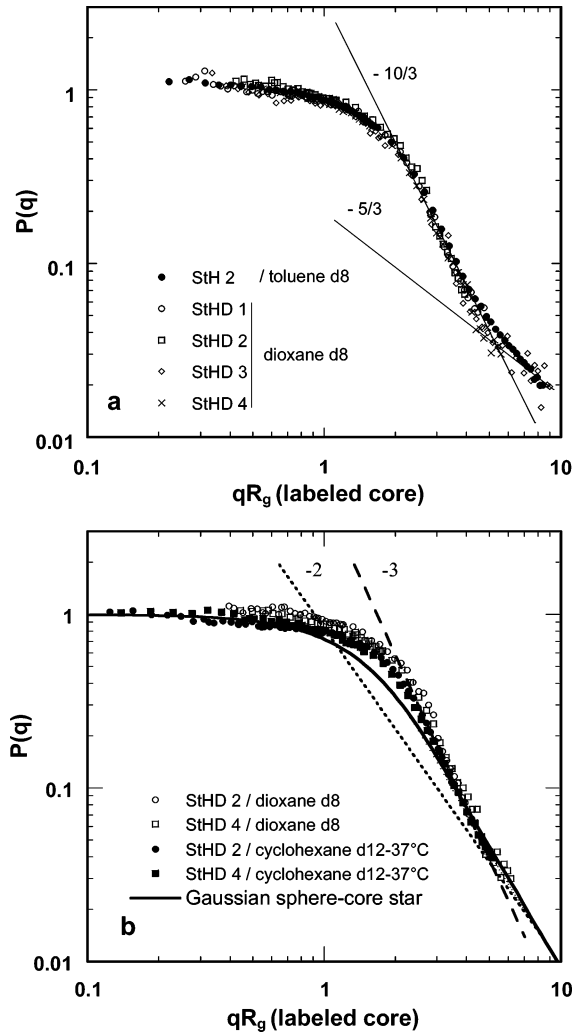

Figure 11. The log−log representation of the form factor of selectively H/D labeled stars StHD: (a) comparison with the scattering behavior of nonlabeled star of nearly equivalent arm length as the labeled species in dioxane-d_8 solutions; (b) comparison with the scattering behavior in cyclohexane-d_{12} solutions (37 °C).

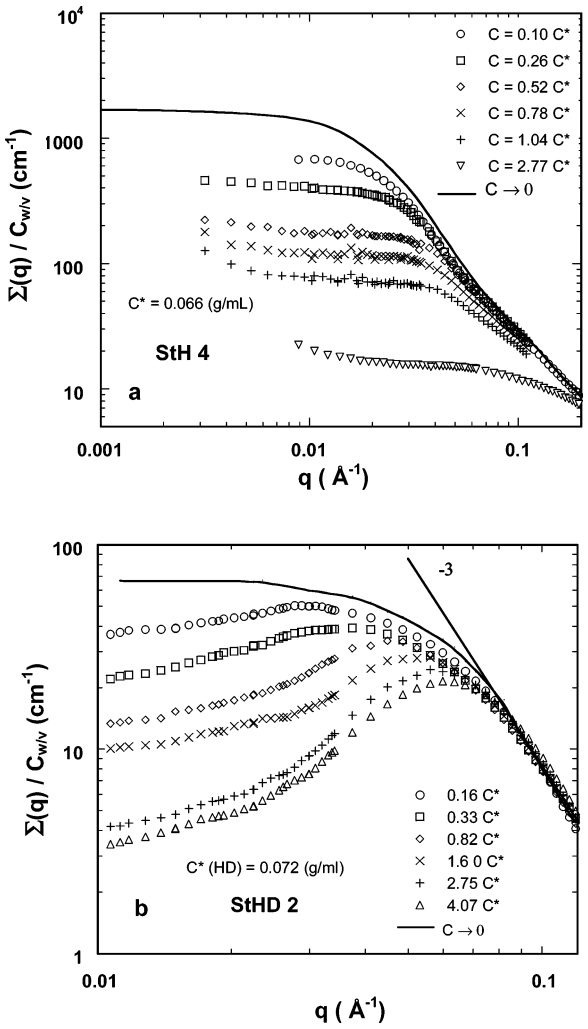

Figure 12. (a) Scattered intensity by non labeled stars (StH4/toluene-d_8) and (b) core labeled stars (StHD2/dioxane-d_8) in semidilute solutions. The whole molecular weight of the stars are nearly equivalent (M_w = 100 000 and 127 000 g/mol respectively) but only the central core of StHD2 (M_w = 21 000 g/mol) contributes to the scattering.

the Zimm plot. The values obtained are in reasonably good agreement with those obtained by L.S. and SEC (Table 4). The variations of the radii of gyration with M_w are presented in Figure 10. In dioxane-d_8 solutions, the mean dimension of the H labeled central star core does not differ from the dimensions of a StH star of equivalent mass. In cyclohexane-d_{12} solutions, a slight decrease is observed as expected in the case of a Θ solvent.

Analysis of the Form Factor. The form factor of the core labeled stars in toluene-d_8 and dioxane-d_8 is shown in Figure 11a, using a standard log−log representation. Because of the small size of the labeled part, reliable experimental results are limited to the Guinier and to the intermediate range of scattering vectors. For the sake of comparison, the form factor of sample StH 2 is also represented, as its molecular weight is close to the central part of the samples StHD1, StHD2, and StHD3. Those last three samples differ in the length of their deuterated sequences. Sample StHD4 has a molecular mass close to StHD3 but differs only by the size of the H labeled central part. Figure 11a shows that, in a good solvent, the chain conformation in the vicinity of the central core is not modified whether these chains are free or linked to long sequences. In cyclohexane-d_{12} (Figure 11b), the intermediate behavior differs slightly from that in dioxane-d_8 solutions, tending toward the one calculated for simple Gaussian stars. Moreover, it should be noted that the slope of the decrease in the intermediate range is close to −3, as expected from the Daoud−Cotton model.[22]

Together, these results are consistent with a monomolecular dispersion of the $C_{60}(PS)_6$ stars with short arms in good solvents such as toluene-d_8 or dioxane-d_8.

2.2. Semidilute Solutions. As mentioned earlier, one of the main purposes of using core labeled stars is to optimize the determination of the structure factor of semidilute polymer stars solutions $S_{int}(q)$. The scattering cross-section can be written as $\Sigma(q) \sim P_{CL}(q)S_{int}(q)$, where $P_{CL}(q)$ is the form factor of the labeled core. The main advantage of this approach is that $P_{CL}(q)$ and $S_{int}(q)$ are separated well beyond the overlapping concentration of the whole star (StHD) C^*_{HD}. Table 4 shows that, for most of the experiments reported here, the overlapping concentration C^*_H of the H-labeled central part of the stars is about five times larger than C^*_{HD}. In these conditions, the scattering contribution of the sea of blobs ξ (c) is contrast matched (see Figure 2). Therefore, the form factor $P_{CL}(q)$ which reflects the structure of the short sequences H attached to the core should not be perturbed by the overlapping of the outer sequences.[22,34,35] Figure 12 displays comparative scattering behaviors of semidilute solutions of StH4 stars in toluene-d_8 and StHD2 stars in dioxane-d_8. Both stars have nearly the same

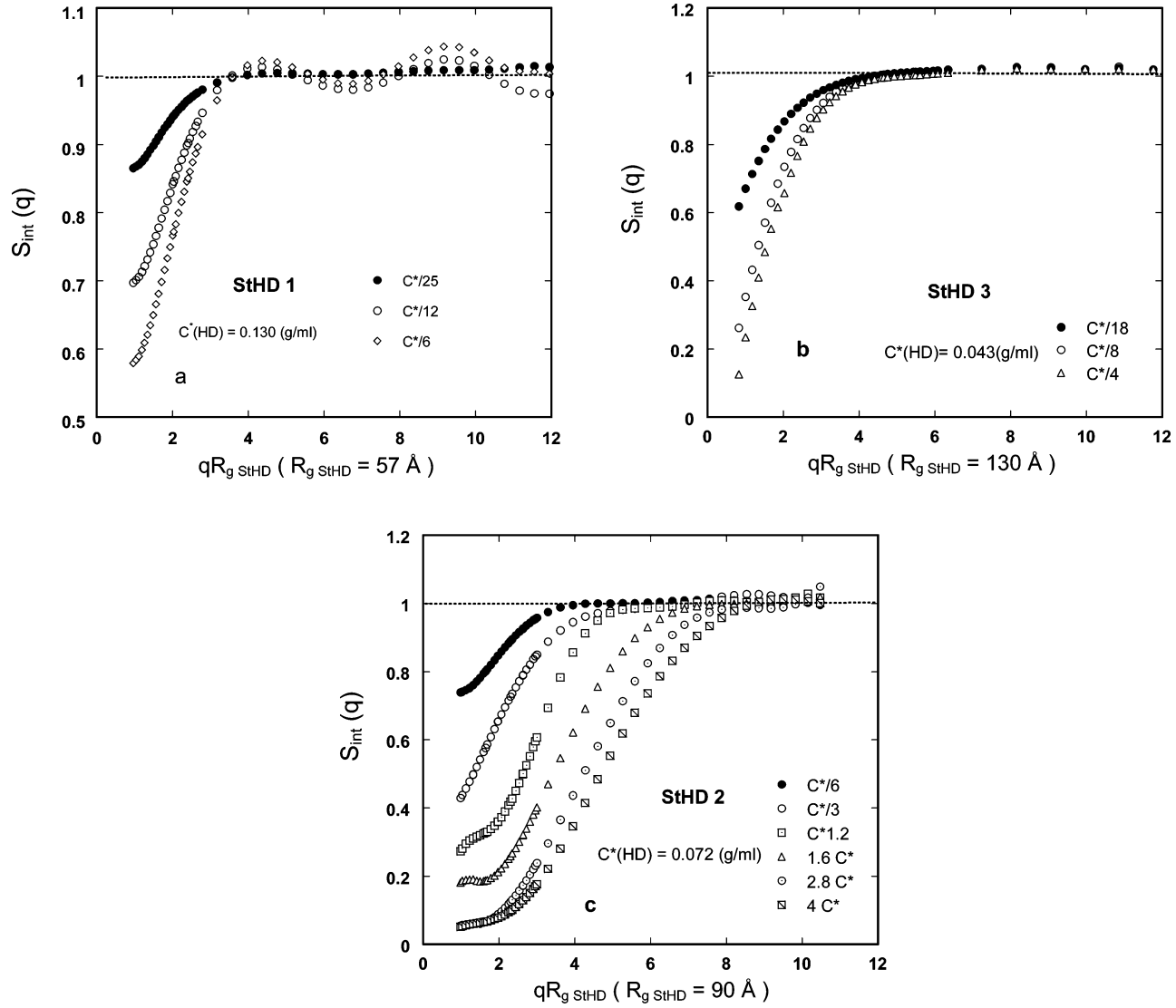

Figure 13. Structure factor $S_{int}(q)$ of StHD stars in semidilute dioxane-d_8 solutions. Effect of the arm length on the spatial ordering: (a) StHD1, $M_{HD} = 64\,000$, $M_H = 12\,600$; (b) StHD3, $M_{HD} = 260\,000$, $M_H = 18\,000$ g/mol. Behavior at higher volume fractions of polymer: (c) StHD2, $M_{HD} = 127\,000$, $M_H = 21\,100$ g/mol.

molecular weight ($M_w \cong 100\,000$), but for StHD2 ($M_w = 21\,000$) only the central H labeled part contributes to the scattering. The two plots in Figure 12 show a strong reduction in the forward scattering, arising from the increase of the osmotic compressibility. As predicted by Witten and Pincus,[43] the osmotic pressure jump is observed in the vicinity of C^*, for both StH 4 and StHD 2. It results from the reduction of the concentration fluctuations near the packing volume fraction. Furthermore, the scattering by the core labeled stars StHD2 shows more clearly the spatial inter-star interactions. Indeed, the observed maximum results predominantly from the structure factor $S_{int}(q)$. It starts to develop for concentrations approaching C^*_{HD} with a q_{max} position in the range $(3-4) \times 10^{-2}$ Å^{-1}. A simple Bragg distance calculation ($d = 2\pi/q_{max}$) leads to $d \cong 180$ Å, which is approximately twice the calculated value of the radius of gyration of the StHD2 star ($R_g \cong 90$ Å). This result comforts the picture of a liquid state order taking place around the overlapping concentration. At high q, and for all the concentrations investigated, the intensities follow the same q decrease ($\sim q^{-10/3}$) resulting from the local contribution of the entangled chains in the vicinity of the fullerene core. This intermediate range of scattering vectors could be attributed to local fluctuations, which are not affected by the inter-star spatial correlation.

In the case of StH4 solutions, the maximum is considerably blurred, both by the contribution of the form factor of this large star and by the scattering of the sea of blobs resulting from the interpenetration of the long sequences. It is mainly for these reasons that the extraction of $S_{int}(q)$ is much more complicated in the case of solutions of nonlabeled star polymer.

The structure factor $S_{int}(q)$ of some semidilute core labeled stars has been evaluated based on $\Sigma(q) \sim P_{CL}(q)S_{int}(q)$. Scattering measurements have been carried out on StHD labeled stars in contrast conditions where the D sequences were matched, and for volume fractions far below C^*_{HD}. Thus, it has been possible to determine with accuracy the extrapolation of $P_{CL}(q)$ at zero concentration. The Figures 13a, b and c display the experimental results obtained on a series of stars with molecular weights of labeled chains linked to the core ranging from 2000 to 3500. The structure factor $S_{int}(q)$ has been plotted as a function of $qR_{g,StHD}$, this last dimension being the calculated radius of gyration of the whole star. At first glance, it can be noted that a spatial correlation between stars emerges far below the overlap concentration of the whole StHD stars. Moreover,

for the lower volume fractions and for the different stars investigated, the structure factor reaches a plateau close to one for values of $qR_{g,\ StHD}$ in the range 3−4. It indicates that the star potential interaction takes place at distances corresponding to about twice the radius of gyration of the stars. $R_{g\ StHD}$ is then the relevant parameter characterizing the inter-star interactions. Figure 13a reveals a peculiar behavior of $S_{int}(q)$ for the sample StHD1 which has a short arm length (nearly 100 monomer units). The structure factor exhibits a weak modulation close to the final plateau reflecting some mutual interaction due to the light coverage of the C_{60} by the short linked chains. These interactions seem to be uniformized by the increase in the concentration. These results are close to those obtained by Dozier,[10] who observed interparticle correlations in poystyrene and polyisoprene star solutions ($f = 12$ and 8) at very low volume fractions (0.03−0.05 times the overlap concentration).

Figure 13b shows that, as the arm length increases, that short distance ordering is no more observed. For much higher arm lengths (StHD 2), no structural ordering appears when the concentration increases above C^*_{HD}, as shown by the plot of $S_{int}(q)$ in Figure 13c.

V. Conclusion

Six-arm polystyrene stars, with a C_{60} core (nonlabeled: StH and selectively H/D labeled: StHD) and molecular weights ranging from 7600 to 2045000 g/mol, have been prepared by addition of "living" PSLi onto the fullerene. The samples of low polydispersity have been characterized by SEC and light scattering, and the molecular parameters have been corroborated by absolute SANS measurements confirming the hexa functionality of the C_{60} polystyrene stars. In good solvent solutions and within the dilute limit, the variation of the mean square radius of gyration as a function of the molecular weight is in good agreement with the results of stars of different chemical species published in the literature.[14] Furthermore, the molecular weight dependence of the $C_{60}(PS)_6$ stars (StH) mean dimensions is in accordance with published results for various stars of equivalent functionality. The analysis of the form factor, which gives an insight into the internal structure of the stars, has been discussed in the framework of the scaling theories. On the basis of a model for stars of high functionality, the scaling theory foresees a standard representation of the form factor as a function of the scaled parameter qR_g for a constant functionality f, whatever the arm length of the stars. Three qR_g ranges, with characteristic power law decrease of the scattering intensity, are foreseen. In this work, we have established that the expected behavior is only observed in the Guinier and in the asymptotic scattering ranges, while in the intermediate part the discrepancy is all the more pronounced as the arm length decreases. That confirms that the scaling approach is no more applicable for hexa functional stars. For stars with the shortest arms (StH1 and StH2), the characteristic excluded volume behavior is not established in the high q range. The structure of the chain in the vicinity of the C_{60} core has been investigated and discussed, using the generalized Kratky representation. A comparison with the core−shell and the broken star models suggests that the sharp and narrow surface of the fullerene core results in a close packing of stretched arm-chains. Scattering by solutions of selectively labeled stars (StHD) in deuterated solvents, matching the contrast of the outer sequence of the arms, has been investigated. In this type of experiment, only the central sequence tethered to the C_{60} core contributes to the scattering. In the dilute solution limit, the results show that, in a good solvent, the mean square dimensions, as well as the scattering form factor of the labeled core of the star StHD, do not differ from that of an equivalent unlabeled star (StH). The conformation of the attached chains in the vicinity of the C_{60} core remains the same whether they are extended or not by longer sequences. In a Θ solvent, a slight decrease of the mean dimensions has been observed. The measurements carried out in semidilute solutions of StHD stars allows to determine the structure factor $S_{int}(q)$, by making a proper use of relation 2. Indeed, it can be asserted that the form factor $P(q)$ of the central labeled sequences is slightly modified far above the overlap concentration of the entire StHD star. Moreover, the outer sequences being contrast matched by the solvent, the contribution of the sea of blobs of these entangled outer sequences is canceled out. Therefore, the evaluation of the structure factor $S_{int}(q)$ by normalization of $\Sigma(q)$ by $P(q)$, in the zero concentration limit, appears to be entirely justified. The results reported in this work show that the representation of $S_{int}(q)$ as a function of the standard parameter $qR_{g,StHD}$ reflects the emergence of inter-star spatial correlations for distances close to twice the mean square radius of gyration of the entire star ($R_{g\ StHD}$). Some ordering has been observed for stars with short arms at volume fraction much lower than the overlap concentration C^*. The overall mutual interaction resulting from the increase in concentration leads to a more uniform liquid-like spatial distribution. For stars with longer arms, $S_{int}(q)$ does not reveal any local ordering even far above the overlap concentration of the StHD star.

As a final comment, these experiments provide information on the conformation and the spatial ordering of polystyrene stars based on C_{60} in solution. In a forthcoming paper, SANS and X-rays experiments carried out on bulk samples will be presented, showing that these well-controlled polymeric derivative of C_{60} are particularly suited for the investigation of the physical properties of bulk nano structured materials based on fullerene.

Acknowledgment. We wish to thank the Institute Laue Langevin and the Laboratoire Leon Brillouin for providing SANS beam time and B. Deme, J. P. Cotton, and A. Brulet for fruitful discussions during the experiments. We are indebted to M. Rawiso for valuable discussions and to H. Benoit for his critical reading of the manuscript.

References and Notes

(1) Samulski, E. T.; DeSimone, J. M.; Hunt, M. O.; Menceloglu, Y., Jr.; Jarnagin, C.; York, G. A.; Labat, K. B.; Wang, H. *Chem. Mater.* **1992**, *4*, 1153.
(2) Wang, C.; Pan, B.; Fu, S. *Macromol. Chem. Phys.* **1996**, *197*, 3783.
(3) Zgonnik, V. N.; Melenevskaya, E. Y.; Litvinova, L. S.; Kever, E. E.; Vinogradova, L. V.; Terent'eva, I. V. *Polym. Sci., Ser. A* **1996**, *38*, 203.
(4) Pantazis, D.; Pispas, S.; Hadjichristidis, N. *J. Polym. Sci., Part A: Polym. Chem.* **2001**, *39*, 2494.
(5) Ederlé, Y.; Mathis, C. *Macromolecules* **1997**, *30*, 2546.
(6) Mathis, C.; Schmaltz, B.; Brinkmann, M. *C. R. Chimie* **2006**, *9*, 1075.
(7) Webber, V.; Duval, M.; Ederlé, Y.; Mathis, C. *Carbon* **1997**, *36*, 839.
(8) Huber, K.; Bantle, S.; Burchard, W.; Fetters, L. J. *Macromolecules* **1986**, *19*, 1404.
(9) Richter, D.; Farago, B.; Fetters, L. J.; Huang, J. S.; Ewen, B. *Macromolecules* **1990**, *23*, 1845.
(10) Dozier, D. W.; Huang, J. S.; Fetters, L. J. *Macromolecules* **1991**, *24*, 2810.
(11) Richter, D.; Jucknischke, L.; Willner, L.; Fetters, L. J.; Lin, M.; Huang, J. S.; Roovers, J.; Toporovsky, P. M.; Zhou, L. L. *J. Phys. IV, Colloq. C8* **1993**, *3*, 3.
(12) Willner, L.; Jucknischke, O.; Richter, D.; Roovers, J.; Zhou, L.-L.; Toporovsky, P. M.; Fetters, L. J.; Huang, J. S.; Lin, M. Y.; Hadjichristidis, N. *Macromolecules* **1994**, *27*, 3821.
(13) Mendes, E.; Lutz, P.; Bastide, J.; Boué, F. *Macromolecules* **1995**, *28*, 174.
(14) Grest, G. S.; Fetters, L. J.; Huang, J. S.; Richter, D. *Adv. Chem. Phys.* **1996**, *94*, 67.

(15) Marques, C. M.; Izzo, D.; Charitat, T.; Mendes, E. *Eur. Phys. J.* **1998**, *3*, 353.
(16) Affholter, K. A.; Henderson, S. J.; Wignall, G. D.; Bunick, G. J.; Haufler, R. E.; Compton, R. N. *J. Chem. Phys.* **1993**, *99*, 9224.
(17) Melnichenko, Y. B.; Wignall, G. D.; Compton, R. N.; Bakale, G. *J. Chem. Phys.* **1999**, *111*, 4724.
(18) Wignall, G. D.; Affholter, K. A.; Bunick, G. J.; Hunt, M. O.; Menceloglu, Y. Z.; DeSimone, J. M.; Samulski, E. T. *Macromolecules* **1995**, *28*, 6000.
(19) Lebedev, V. T.; Török, G.; Cser, L.; Zgonnik, V. N.; Budtov, V. P.; Brulet, A.; Vinogradova, L. V.; Melenevskaya, E. Y.; Orlova, D. N.; Sibilev, A. I. *Physica B* **2000**, *402*, 276−278.
(20) Török, G.; Lebedev, V. T.; Bershtein, V. A.; Zgonnik, V. N. *J. Non-Cryst. Solids* **2002**, *705*, 307−310.
(21) Lebedev, V. T.; Török, G.; Vinogradova, L. V.; Orlova, D. N.; Melenevskaya, E. Y.; Zgonnik, V. N.; Treimer, W. *Fullerenes, Nanotubes, Carbon Nanostruct.* **2004**, *1 & 2*, 377.
(22) Daoud, M.; Cotton, J. P. *J. Phys.* **1982**, *43*, 531.
(23) Szwarc, M. *Carbanions, Living Polymers and Electron Transfer Processes*; Wiley-Interscience; New York, 1968.
(24) Ruoff, R. S.; Doris, S.; Malhotra, R.; D. C. Lorents, D. C. *J. Phys. Chem.* **1993**, *97*, 3379.
(25) Higgins, J. S.; Benoit, H. C. *Polymers and Neutron Scattering*; Clarendon Press: Oxford, U.K., 1994.
(26) Strazielle, C.; Benoit, H. *Macromolecules* **1975**, *2*, 203.
(27) Benoit, H.; Decker, D.; Higgins, J. S.; Picot, C.; Cotton, J. P.; Farnoux, B.; Jannink, G.; Ober, R. *Nature Phys. Sci.* **1973**, *140*,13.
(28) Benoit, H. *J. Polym. Sci.* **1953**, *11*, 507.
(29) Benoit, H.; Joanny, J. F.; Hadziioannou, G.; Hammouda, B. *Macromolecules* **1993**, *26*, 5790.
(30) Ionescu, L.; Picot, C.; Duval, M.; Duplessix, R.; Benoit, H.; Cotton, J. P. *J. Polym. Sci., Polym. Phys. Ed.* **1981**, *19*, 1019.
(31) Kotaka, T.; Tanaka, T.; Hattori, M.; Inagaki, H. *Macromolecules* **1978**, *11*, 138.
(32) Pedersen, J. S.; Gerstenberg, M. C. *Macromolecules* **1996**, *29*, 1363.
(33) Pedersen, J. S. *Adv. Colloid Interface Sci.* **1997**, *70*, 171.
(34) Birshtein, T.; Zhulina, E. B. *Polymer* **1984**, *25*, 1453.
(35) Birshtein, T.; Zhulina, E. B.; Borisov, O. V. *Polymer* **1986**, *27* 1078.
(36) Allessandrini, J. L.; Carignano, M. A. *Macromolecules* **1992**, *25*, 1157.
(37) Grest, G. S.; Murat, M. *Monte Carlo and Molecular Dynamics Simulations in Polymer Science*; Binder, K., Ed., Clarendon Press: Oxford, U.K., 1995.
(38) Grest, G. S.; Kremmer, K.; Witten, T. A. *Macromolecules* **1987**, *20*, 1376.
(39) Allegra, G.; Colmbo, E.; Ganazolly, F. *Macromolecules* **1993**, *26*, 330.
(40) Allegra, G.; De Vitis, M.; Ganazolly, F. *Makromol. Chem. Chem. Theory Simulation* **1993**, *2*, 829.
(41) Auvray, L. *C. R. Acad. Sci. Paris* **1986**, *302 II*, 859.
(42) Auvray, L.; de Gennes, P. G. *Europhys. Lett.* **1986**, *2*, 647.
(43) Witten, T. A.; Pincus, P. A. *Macromolecules* **1986**, *19*, 2509.
(44) Ruelle, P.; Farina-Cuendet, A.; Kesserling, U. W. *J. Am. Chem. Soc.* **1996**, *118*, 1777.
(45) Rahlwes, D.; Kirste, R. G. *Makromol. Chem.* **1977**, *178*, 1793.
(46) Huber, K.; Burchard, W. *Macromolecules* **1989**, *22*, 3332.

MA060557K